

ARTICLE

Received 16 Dec 2011 | Accepted 19 Mar 2012 | Published 24 Apr 2012

DOI: 10.1038/ncomms1795

Distinct Nav1.7-dependent pain sensations require different sets of sensory and sympathetic neurons

Michael S. Minett¹, Mohammed A. Nassar², Anna K. Clark³, Gayle Passmore¹, Anthony H. Dickenson⁴, Fan Wang⁵, Marzia Malcangio³ & John N. Wood¹

Human acute and inflammatory pain requires the expression of voltage-gated sodium channel Nav1.7 but its significance for neuropathic pain is unknown. Here we show that Nav1.7 expression in different sets of mouse sensory and sympathetic neurons underlies distinct types of pain sensation. Ablating Nav1.7 gene (*SCN9A*) expression in all sensory neurons using Advillin-Cre abolishes mechanical pain, inflammatory pain and reflex withdrawal responses to heat. In contrast, heat-evoked pain is retained when *SCN9A* is deleted only in Nav1.8-positive nociceptors. Surprisingly, responses to the hotplate test, as well as neuropathic pain, are unaffected when *SCN9A* is deleted in all sensory neurons. However, deleting *SCN9A* in both sensory and sympathetic neurons abolishes these pain sensations and recapitulates the pain-free phenotype seen in humans with *SCN9A* loss-of-function mutations. These observations demonstrate an important role for Nav1.7 in sympathetic neurons in neuropathic pain, and provide possible insights into the mechanisms that underlie gain-of-function Nav1.7-dependent pain conditions.

¹ Molecular Nociception Group, WIBR UCL, Gower Street, London WC1E 6BT, UK. ² Department of Biomedical Science, The University of Sheffield, Western Bank, Sheffield S10 2TN, UK. ³ Wolfson Centre for Age-Related Diseases, King's College London, Guy's Campus, London Bridge, London SE1 1UL, UK. ⁴ Department of Pharmacology, University College London, Gower Street, London WC1E 6BT, UK. ⁵ Department of Cell Biology and Department of Neurobiology, Duke University Medical Center, Durham, North Carolina 27710, USA. Correspondence and requests for materials should be addressed to J.N.W. (email: j.wood@ucl.ac.uk).

Voltage-gated sodium channels are crucial determinants of neuronal excitability and signalling. Voltage-gated sodium channels Nav1.7, 1.8 and 1.9 are expressed in peripheral neurons and have been linked to pain pathways¹. The biophysical characteristics of Nav1.7 suggest a role in initiating action potentials in response to depolarization of sensory neurons by noxious stimuli^{2,3}. Nav1.8 is a major contributor to the upstroke of action potentials in sensory neurons and is essential for cold pain perception⁴. Nav1.9 influences inflammatory pain thresholds by producing a persistent current that helps determine the resting membrane potential⁵.

Rare human genetic conditions involving Nav1.7 mutations demonstrate its important role in pain pathways. Dominant gain-of-function mutations can cause primary erythromelalgia, resulting in burning pain and flushing⁶. Mutations associated with the condition, for example F1449V⁷ and L858H⁸, result in lower thresholds for action potential firing and higher-frequency firing in sensory neurons. Other gain-of-function Nav1.7 mutations that cause defective fast inactivation may cause burning pain associated with paroxysmal extreme pain disorder (PEPD), in which mechanical stimulation triggers pain⁹. Loss-of-function recessive mutations cause congenital insensitivity to pain (CIP) and anosmia; individuals with this syndrome are of normal intelligence and can function effectively^{3,10}. These observations highlight Nav1.7 as a potentially useful target for the development of novel analgesics.

Early studies on Nav1.7 function in transgenic mice focused on the role of this channel in Nav1.8-positive nociceptors¹¹. Deletion of the *SCN9A* gene in these neurons results in a loss of sensitivity to high-threshold noxious mechanical stimuli and major deficits in inflammatory pain. Unlike humans with global loss-of-function mutations, however, there is no deficit in noxious thermosensation. Here we have used Cre recombinase expressed in different sets of sensory and sympathetic neurons to explore modality-specific pain

sensations that are dependent on the expression of Nav1.7. Advillin is an actin-binding protein that is selectively expressed within all trigeminal and dorsal root ganglion (DRG) neurons^{12,13}. We used Cre driven by the Advillin promoter to delete Nav1.7 in all sensory neurons¹⁴, and compared phenotypes with mice in which Nav1.7 is deleted using Cre driven by Nav1.8 in a subpopulation of sensory neurons (*Nav1.7^{Nav1.8}*)¹¹. Wnt1 is expressed in neural crest cells that are the precursors of sensory and autonomic neurons¹⁵. This has allowed us to exploit a Wnt1-Cre mouse¹⁶ to examine the contribution of Nav1.7 to pain behaviour in both the sensory and sympathetic neurons, where it is selectively expressed¹⁷. We have thus been able to define the pain modalities associated with different sets of peripheral neurons that express Nav1.7. We provide evidence that Nav1.7 may be involved at both the central as well as the peripheral terminals of sensory neurons in pain signalling. We also demonstrate an interaction between sympathetic and primary sensory neurons in acute heat sensing as well as neuropathic pain, which are both dependent upon Nav1.7 activity. These experiments provide a comprehensive mouse model of human CIP for mechanistic studies and reinforce the significance of Nav1.7 as an analgesic drug target.

Results

Pan-DRG neuron gene ablation with an Advillin-Cre mouse. The expression pattern of functional Cre was first examined by crossing an Advillin-Cre knock-in-positive mouse line¹⁴ with Rosa26 floxed-stop β -galactosidase-expressing reporter mice¹⁸. X-gal staining of E14.5 Advillin-Cre-positive reporter (*Advillin-Cre^{+/+}*) mice embryos showed that Cre expression is confined to the DRG and trigeminal neurons (Fig. 1a,b), while no staining is seen in Advillin-Cre-negative reporter mice. Positive X-gal staining was seen in all DRG cells in sections taken from 6-week-old *Advillin-Cre^{+/+}* reporter mice (Fig. 1c). No positive staining was seen in other

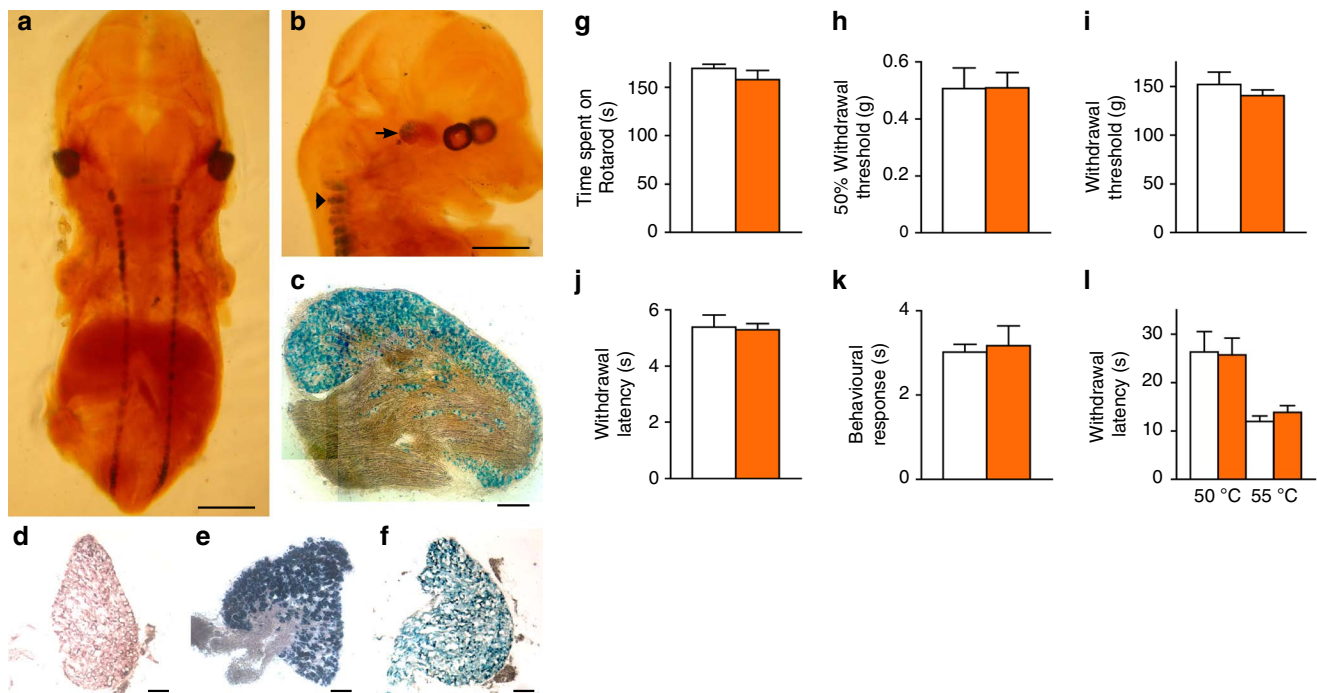


Figure 1 | Advillin and Wnt1 Cre expression pattern and pain behaviour of Advillin-Cre mice. (a,b) Expression pattern of Cre activity. Arrow: trigeminal, arrowhead: DRG (scale bar 1 mm). X-gal staining of Advillin-Cre positive (c) DRG and (d) SCG sections, and Wnt1-Cre positive (e) DRG and (f) SCG sections (scale bar 100 μm). Acute nociceptive responses of heterozygous Advillin-Cre (orange columns) and littermate (white columns) mice (N shown as littermate/Advillin-Cre^{+/+}). (g) Motor coordination: Rotarod test (N = 15/16). (h) Light touch: von Frey (N = 15/16). (i) Mechanical pain: Randall-Selitto test (N = 13/16). (j) Thermal spinal reflex: Hargreaves' test (N = 15/16). (k) Noxious cooling: acetone test (N = 10/11). (l) Supraspinal thermal: hotplate test at 50 and 55 °C (N = 6/6). All behavioural data analysed by *t*-test. Results are presented as mean ± s.e.m.

tissues sampled, including the superior cervical ganglia (SCG—Fig. 1d). This X-gal staining seen in *Advillin-Cre*^{+/-} reporter mice corroborates previous studies of expression patterns using *in situ* hybridization and human placental alkaline phosphatase reporter mice¹². The expression pattern of *Wnt1-Cre* has been reported¹⁶, and was confirmed by crossing *Wnt1-Cre*-positive mice with Rosa26 floxed-stop β -galactosidase reporter mice. Positive X-gal staining was seen in both DRG and SCG isolated from *Wnt1-Cre*-positive reporter mice (Fig. 1e,f). A count of cells with positive staining for antibodies to neurofilament N200 protein (a marker of A-fibre-associated sensory neurons—Supplementary Fig. S1a,b) as well as peripherin (a marker of nociceptive sensory neurons—Supplementary Fig. S1a,b) shows no neuronal loss in *Advillin-Cre*^{+/-} mice (Supplementary Fig. S1c).

Having established that *Advillin-Cre* was effective in deleting genes in all sensory neurons, we examined the behaviour of the *Advillin-Cre* mouse line. Motor function was assessed using the Rotarod test¹⁹, which showed that the responses of *Advillin-Cre*^{+/-} mice are the same as those of wild-type littermate controls (Fig. 1g). Mechanosensation assessed using von Frey filaments applied to the hindpaw and the Randall–Selitto test applied to the tail also showed normal responses in *Advillin-Cre*^{+/-} mice (Fig. 1h,i). Finally, pain behaviour in response to noxious thermal stimuli applied to the hindpaw(s) was also normal (Fig. 1j–l). Behavioural responses to both short- and long-term inflammatory pain models were also normal in *Advillin-Cre*^{+/-} mice (Fig. 2a–e). Similarly, mechanical sensitivity developed normally in response to surgically induced neuropathic pain (Fig. 2f). The same acute pain tests as described above were performed on *Wnt1-Cre*-expressing mice, which showed responses similar to wild-type littermate controls (Supplementary Fig. S2a–f). *Wnt1-Cre* mice have previously been shown to have normal behavioural responses in both inflammatory and neuropathic pain models²⁰. Thus, there are no background problems in interpreting behavioural phenotypes when using these mice for gene deletion studies.

Polymerase chain reaction (PCR) analysis showed that *SCN9A* exons 14 and 15 are deleted in cDNA isolated from DRG in homozygous floxed *SCN9A*, *Advillin-Cre*^{+/-} mice (*Nav1.7^{Advill}*) but not in the littermate homozygous floxed *SCN9A* *Advillin-Cre*-negative mice (Supplementary Fig. S3a). However, exons 14 and 15 remain intact in the SCG that contain the cell bodies of sympathetic neurons in *Nav1.7^{Advill}* mice (Supplementary Fig. S3b). In contrast, exons 14 and 15 are deleted in cDNA isolated from both DRG and SCG (Supplementary Fig. S3c,d) in the homozygous floxed *SCN9A*, *Wnt1-Cre*-positive mice (*Nav1.7^{Wnt1}*).

Nav1.7 knockout mice define pain modality-specific neurons.

By comparing the pain behaviour of different mouse lines, it was possible to examine the role of Nav1.7 expressed in Nav1.8-positive sensory neurons (*Nav1.7^{Nav1.8}*), all sensory neurons (*Nav1.7^{Advill}*) or sensory and sympathetic neurons (*Nav1.7^{Wnt1}*). Analysis of the behavioural responses of *Nav1.7^{Nav1.8}*, *Nav1.7^{Advill}* and *Nav1.7^{Wnt1}* mice in a number of different pain models showed that their pain phenotypes differ. Fig. 3a shows that all three Nav1.7 knockout mouse strains show pronounced analgesia in terms of noxious mechanosensation measured with a Randall–Selitto apparatus, when compared with their littermate controls. This confirms the findings of Nassar *et al.*¹¹, who examined the *Nav1.7^{Nav1.8}* mouse. The Randall–Selitto test results suggest that deleting Nav1.7 within Nav1.8-positive DRG neurons is sufficient to abolish responses to mechanical pain. However, the results of the acetone (noxious cooling) test (Fig. 3b) and Hargreaves' (thermal: spinal withdrawal reflex) test (Fig. 3c) show deficits in the *Nav1.7^{Advill}* and *Nav1.7^{Wnt1}* mice, while the behavioural response of *Nav1.7^{Nav1.8}* was not significantly different from littermate controls (confirmed by separate behavioural tests—Supplementary Fig. S4a,b). Thus, noxious cooling-evoked

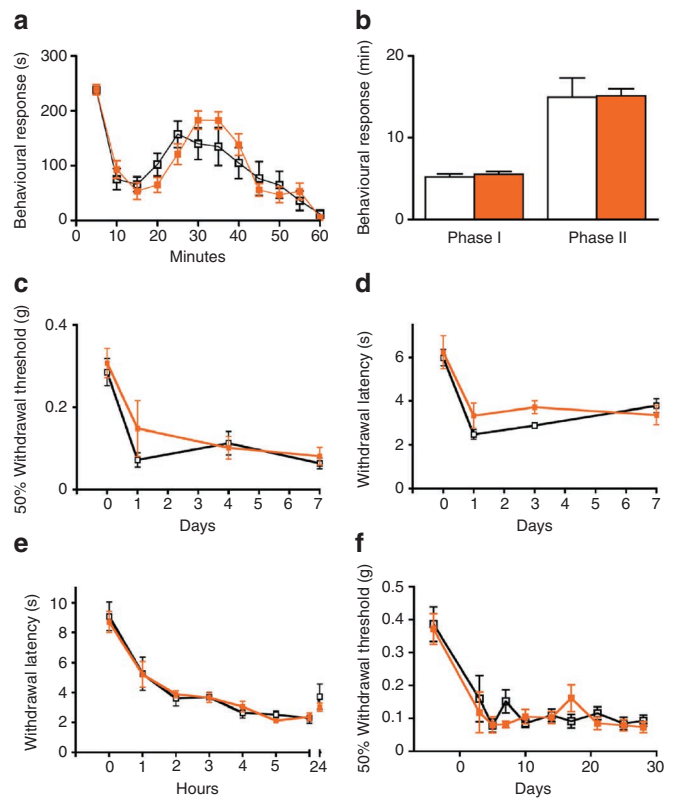


Figure 2 | Advillin-Cre does not affect inflammatory or neuropathic pain behaviour. *Advillin-Cre*^{+/-} (orange boxes/columns), littermates (white boxes/columns). **(a,b)** Behavioural responses of *Advillin-Cre*^{+/-} (*N* = 12) wild-type littermate (*N* = 8) mice following intraplantar injection of 20 μ l of 5% formalin. **(c)** von Frey 50% threshold response of *Advillin-Cre*^{+/-} (*N* = 9) and wild-type littermate (*N* = 8) mice following intraplantar injection of 20 μ l of complete Freund's adjuvant. **(d)** Hargreaves' test responses of *Advillin-Cre*^{+/-} mice (*N* = 9) and wild-type littermate (*N* = 8) mice following intraplantar injection of 20 μ l of complete Freund's adjuvant. **(e)** Hargreaves' test response of *Advillin-Cre*^{+/-} mice (*N* = 12) and wild-type littermates (*N* = 10) mice following intraplantar injection of 20 μ l of carrageenan. **(f)** von Frey 50% threshold response of *Advillin-Cre*^{+/-} mice (*N* = 12) and wild-type littermates (*N* = 10) mice following L5 SNT. All data analysed by two-way analysis of variance followed by the Bonferroni *post hoc* test. Results are presented as mean \pm s.e.m.

behaviour and spinal withdrawal reflexes to noxious heat require Nav1.7 expression in Nav1.8-negative sensory neurons. However, this is not true for supraspinal responses to the hotplate test (Fig. 3d—discussed below). Other work supports the view that Nav1.7 expressed within Nav1.8-positive DRG neurons contributes little to thermal nociceptive processing. Abrahamsen *et al.*²¹ showed that behavioural responses to noxious thermal stimuli (with the exception of extreme cold) remain intact in mice in which all Nav1.8-positive neurons have been ablated with diphtheria toxin (*Nav1.8^{DTA}*). Additionally, *in vivo* electrophysiological recordings from spinal lamina V wide dynamic range (WDR) neurons in *Nav1.7^{Advill}*, *Nav1.7^{Nav1.8}* and *Nav1.8^{DTA}* mice corroborate the behavioural data. Critically, WDR responses in *Nav1.7^{Advill}* mice show that both noxious heat and mechanical stimuli are attenuated (Fig. 3e,f). In contrast, only mechanically evoked and not heat-evoked WDR responses are attenuated in both *Nav1.7^{Nav1.8}* mice¹¹ and *Nav1.8^{DTA}* mice²¹. This demonstrates clearly that Nav1.7 expressed in Nav1.8-positive DRG neurons is essential for processing noxious mechanical stimuli while Nav1.7 in Nav1.8-negative DRG neurons is essential for processing noxious thermal stimuli.

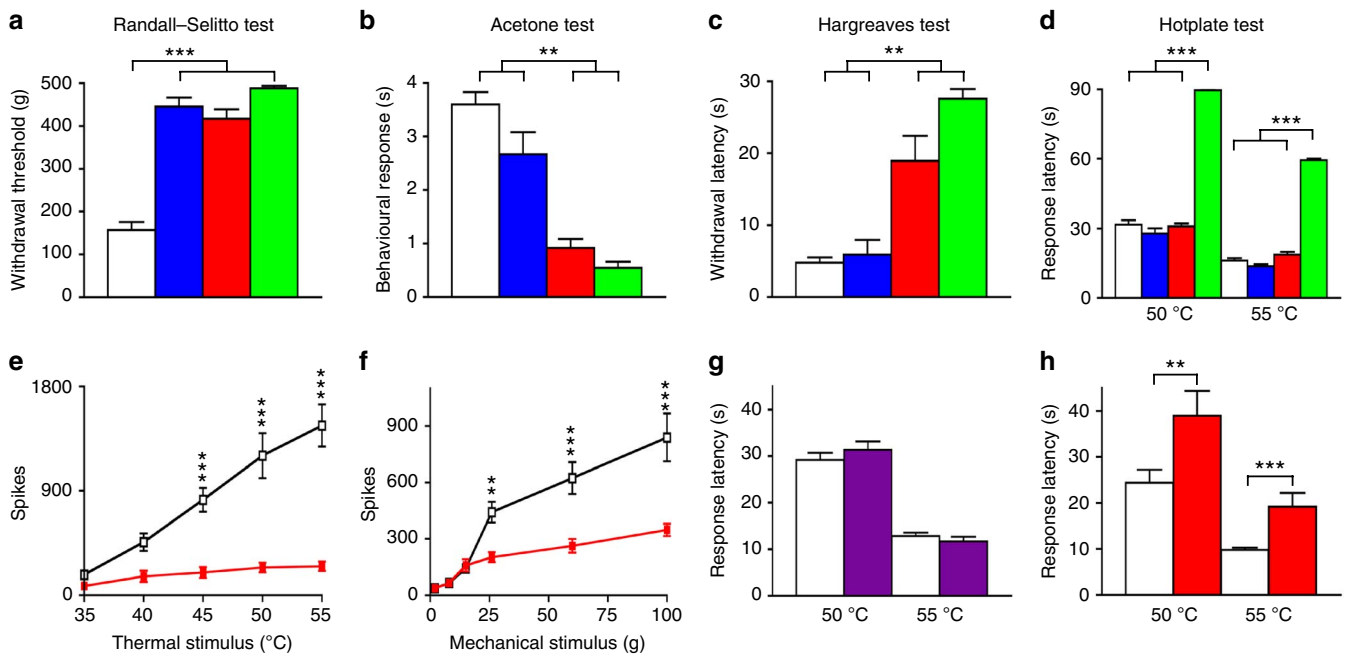


Figure 3 | Nociceptive responses of different tissue-specific Nav1.7 KO mice. Littermate (white columns), Nav1.7^{Nav1.8} (blue columns), Nav1.7^{Advill} (red columns) and Nav1.7^{Wnt1} (green columns), N shown as littermate/Nav1.7^{Nav1.8}/Nav1.7^{Advill}/Nav1.7^{Wnt1}. **(a)** Randall-Selitto test (noxious mechanical stimulus; $N = 23/6/13/5$). **(b)** Acetone cooling test (noxious cooling stimulus; $N = 29/6/7/5$). **(c)** Hargreaves' test (spinal noxious heat stimulus; $N = 22/6/7/7$). **(d)** Hotplate test (supraspinal noxious heat stimulus; $N = 37/8/19/10$): *in vivo* electrophysiological spinal cord recording from Nav1.7^{Advill} (red boxes) and littermate (white boxes) mice. **(e)** Thermally evoked WDR responses ($N = 6$ per group). **(f)** Mechanically evoked WDR responses ($N = 6$ per group). **(g)** Hotplate test following 6-OHDA treated (purple column, $N = 10$) and untreated (white column, $N = 12$) C57/Black6 mice. **(h)** Hotplate test of Nav1.7^{Advill} (red column, $N = 7$) and littermate mice (white column, $N = 12$) following chemical 6-OHDA treatment. **(a-d)** Data analysed by *t*-test, **(e-h)** data analysed by two-way analysis of variance followed by the Bonferroni *post hoc* test. Results are presented as mean \pm s.e.m. ** $P < 0.01$ and *** $P < 0.001$ (individual points).

Nav1.7 is expressed in sympathetic as well as sensory neurons^{2,17}. By using the Wnt1 promoter to drive Cre expression it is possible to delete genes in neural crest derivatives including autonomic and sensory neurons. Therefore, we could identify any role for Nav1.7 in sympathetic neurons by comparing the phenotype of Nav1.7^{Advill} and Nav1.7^{Wnt1} mice. Interestingly, only Nav1.7^{Wnt1} mice have an attenuated response to the hotplate test (Fig. 3d), which is a measure of supra-spinal responses²² to damaging thermal stimuli rather than a spinal reflex involving only cells in the spinal cord²³. In contrast, Nav1.7^{Advill} (as well as Nav1.7^{Nav1.8}) mice show normal hotplate pain behaviour (Fig. 3d). However, this does not mean that Nav1.7 in sympathetic neurons alone confers sensitivity to the hotplate test. Chemical sympathectomy using 6-hydroxydopamine (6-OHDA)²⁴ in wild-type mice has no effect on behavioural responses to the hotplate test (Fig. 3g) or any other acute pain thresholds tested (Supplementary Fig. S5a-f). However, when chemical sympathectomy is combined with the deletion of sensory neuron Nav1.7 in Nav1.7^{Advill} mice, the hotplate response is diminished (Fig. 3h). Thus, only when Nav1.7 expression is lost in both sensory and sympathetic neurons do mice become unresponsive (Fig. 3d). Despite the role of the sympathetic nervous system in thermoregulation, the core temperature and skin temperature of Nav1.7^{Wnt1} (Fig. 4a) and 6-OHDA-treated mice (Supplementary Fig. S5g) were found to be normal.

We next examined the responses of the three Nav1.7 knockout lines to noxious cold stimuli, and compared them with a global Nav1.8 knockout mouse that is known to lose sensitivity to noxious cold⁴. Interestingly, the Nav1.8 knockout mouse responded to acetone-induced cooling in the same way as littermate control mice (Fig. 4b), but showed an attenuated response to extreme cold (Fig. 4c). In contrast, all three Nav1.7 conditional knockout mouse

lines that showed attenuated responses to acetone-induced cooling (Fig. 3b) avoided extreme cold like their littermate controls (Fig. 4d). Thus, noxious cold sensation is not Nav1.7 dependent. Finally, all three Nav1.7 knockout mouse lines showed normal responses to light touch and motor coordination (Fig. 4e,f), reinforcing the link between Nav1.7 and pain rather than innocuous somatosensation.

Substance P release from DRG neurons is Nav1.7 dependent. The functional consequences of deleting Nav1.7 in DRG neurons were further examined electrophysiologically. Nav1.7^{Advill} DRG neurons showed a significant average reduction in tetrodotoxin (TTX)-sensitive sodium current amplitude, whereas TTX-resistant sodium currents were unchanged (Fig. 5a). Complete current-voltage relationships are shown in Fig. 5b,c. Approximately 30% of small DRG neurons have been shown to be electrically silenced by the deletion of Nav1.7 in Nav1.8-positive DRG neurons²⁵. We found that electrically stimulated polysynaptic peripheral input into spinal lamina V WDR neurons no longer resulted in wind-up (Fig. 5d)—an *N*-methyl-D-aspartate receptor-mediated form of long-term sensitization that requires substance P release from sensory neurons²⁶. Substance P release from sensory neurons was therefore measured in Nav1.7^{Advill} mice. Strikingly, electrical stimulation of isolated sciatic nerve roots failed to induce increased substance P release into the dorsal horn of Nav1.7^{Advill} mice (Fig. 5e).

The deficits in sensory neuron function and lack of wind-up may be related to pain behaviour assessed using the formalin test. This comprises a first phase of paw licking driven by nociceptor activation followed by a second phase associated with spinal cord hypersensitivity mediated by chemical messengers including substance P²⁷. Nav1.7^{Advill} mice show a striking ~75% decrease in

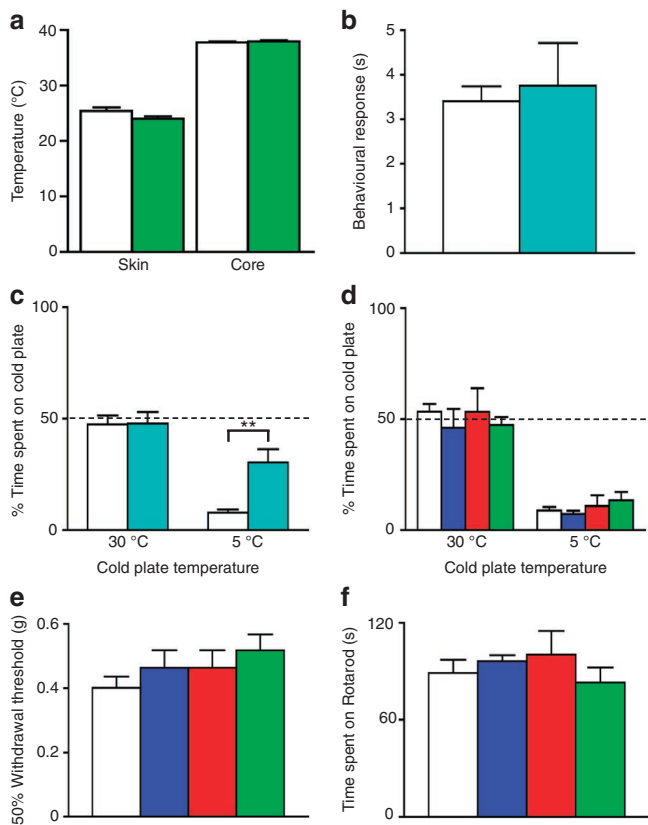


Figure 4 | Behavioural responses of different tissue-specific Nav1.7 and Nav1.8 KO mice to cooling and extreme cold. N shown as littermate/Nav1.7^{Wnt1}. **(a)** Nav1.7^{Wnt1} (green columns) and littermate (white columns) core ($N=12/13$) and skin temperature ($N=12/9$). **(b)** Behavioural response of Nav1.8 KO (turquoise column, $N=5$) and littermate (white column, $N=7$) mice to the acetone cooling test. **(c)** Behavioural response of Nav1.8 KO (turquoise columns, $N=8$) and littermate (white columns, $N=6$) thermal place preference test. **(d-f)** Littermate (white columns), Nav1.7^{Nav1.8} (blue columns), Nav1.7^{Advill} (red columns), Nav1.7^{Wnt1} (green columns) N shown as littermate/Nav1.7^{Nav1.8}/Nav1.7^{Advill}/Nav1.7^{Wnt1}. **(d)** Behavioural response of all three Nav1.7 tissue-specific knockout mice to thermal place preference test ($N=15/8/8/8$). **(e)** Behavioural response of all three Nav1.7 tissue-specific knockout mice to the von Frey test. **(f)** Behavioural response of all three Nav1.7 tissue-specific knockout mice to the Rotarod test ($N=23/8/13/9$). **(a,b)** Data analysed by t-test, **(c-f)** data analysed by two-way analysis of variance followed by the Bonferroni *post hoc* test. Results are presented as mean \pm s.e.m. $**P < 0.01$ (individual points).

behavioural responses during phase II of the formalin test (Fig. 5f), which is similar to the phase II phenotype of both Nav1.7^{Nav1.8} and Nav1.8^{DTA} mice^{11,21}.

Interestingly, Nav1.7^{Advill} mice show a large phase I behavioural deficit (~50% decrease in behavioural responses) whereas Nav1.7^{Nav1.8} mice¹¹ and Nav1.8^{DTA} mice²¹ do not. This suggests an important role for Nav1.7 expressed in Nav1.8-negative DRG neurons during the initial nociceptive phase of the formalin test²⁶.

Neuropathic pain requires Nav1.7 in sympathetic neurons.

Previously Nassar *et al.*¹¹ showed that Nav1.7^{Nav1.8} mice develop neuropathic pain normally. Thus, Nav1.7 expressed in Nav1.8-positive neurons, while making a major contribution to inflammatory pain, does not contribute to neuropathic pain¹¹. Importantly, Nav1.8^{DTA} mice also develop neuropathic pain normally, showing that Nav1.8-positive neurons are not required

for the development of neuropathic pain²⁸. However, recently a blocker of inactivated Nav1.7 has been claimed to reverse mechanical hyperalgesia associated with neuropathic pain models²⁸. This suggests a possible contribution to neuropathic pain of Nav1.7 expressed in Nav1.8-negative DRG neurons, which remain intact within Nav1.7^{Nav1.8} mice. Therefore, Nav1.7^{Advill} mice in which Nav1.7 is lost in all sensory neurons were examined. Nav1.7^{Advill} mice developed mechanical hypersensitivity to the same extent as normal littermates, following spinal nerve transection (SNT) at the fifth lumbar segment—a model of neuropathic pain^{29–31} (Fig. 6a). Thus, Nav1.7 in sensory neurons is not required for the development of neuropathic pain. In contrast, Nav1.7^{Wnt1} mice show a pronounced attenuation in the development of mechanical sensitization and return to baseline behaviour ($\pm 10\%$) within 10 days following surgery (Fig. 6b). This set of observations demonstrate that Nav1.7 expression in sympathetic neurons is essential for the establishment of neuropathic pain. An important role for sympathetic neurons in neuropathic pain is further demonstrated by the ability of a chemical sympathectomy to partially alleviate mechanical hypersensitivity in Nav1.7^{Wnt1} littermate mice following SNT (Fig. 6c). In these experiments, neuropathic pain was established for 28 days, followed by chemical sympathectomy. A substantial, if incomplete, reversal of mechanical hypersensitivity was observed consistent with a sympathetic sensory interaction contribution to the establishment of neuropathic pain. These results may help explain the apparent utility of Nav1.7 antagonists in treating neuropathic pain²⁷.

Discussion

The apparently normal phenotype of humans with SCN9A loss-of-function mutations, apart from anosmia and loss of pain sensation, has focused attention on Nav1.7 as a plausible analgesic drug target. Ablation of the channel using the Cre-loxP system in mice leads to silencing of a significant set of sensory neurons²⁵. We found that TTX-sensitive current densities were reduced in sensory neurons that no longer express Nav1.7. More surprisingly, we found that substance P release into the dorsal horn of the spinal cord evoked by electrical stimulation was completely abolished in the absence of Nav1.7, leading to a loss of wind-up and centrally mediated pain sensitization. In the olfactory system, Weiss *et al.*¹⁰ have shown that while olfactory neurons support action potential propagation in the absence of Nav1.7, the release of neurotransmitter from olfactory neurons is completely abolished, leading to anosmia. A similar deficit may occur in DRG sensory neurons. Thus, Nav1.7 may contribute to pain signalling by DRG neurons in three ways: (1) by recruiting Nav1.8 to transmit noxious input into the spinal cord^{1,2}; (2) by supporting action potential propagation^{25,32} and (3) by regulating neurotransmitter release at central terminals¹⁰.

In terms of responses to innocuous stimuli and motor function, the ablation of Nav1.7 in all sensory and sympathetic neurons is without effect (Fig. 4e,f). However, threshold withdrawal behavioural responses to noxious pressure require Nav1.7 in a set of sensory neurons that express Nav1.8. This corroborates previous findings in Nav1.7^{Nav1.8} mice¹¹ and Nav1.8^{DTA} mice²¹. Reflex threshold withdrawal responses to noxious heat are dependent on Nav1.7 expression in a different set of sensory neurons that do not express Nav1.8, an observation consistent with cell ablation studies²¹. Noxious cold is the sole pain modality that is Nav1.7 independent (Fig. 4d), confirming a previously described role for Nav1.8, which is sensitized at low temperatures⁴ (Fig. 4c). Responses to noxious cooling associated with the application of acetone, however, are not dependent on Nav1.8 (Fig. 4b), but depend upon Nav1.7 expression in Nav1.8-negative sensory neurons.

Acute pain has a clear survival function. Inflammatory pain has a positive role in enhancing self-protection and wound healing, but may cause considerable suffering in chronic inflammatory

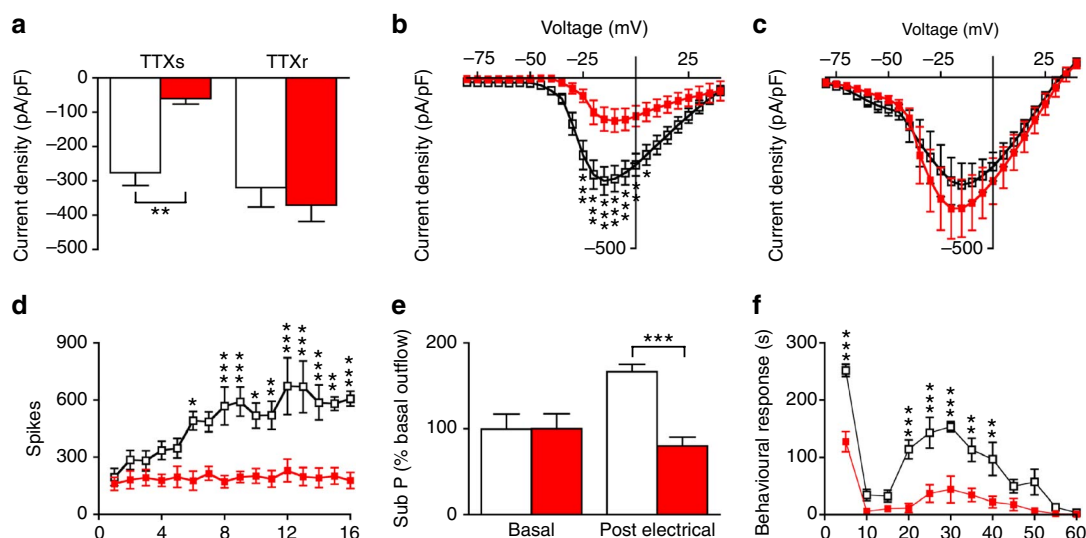


Figure 5 | Reduced electrically evoked wind-up and substance P release in the spinal cord of Nav1.7^{Advill} mice. Littermate (white columns/boxes), Nav1.7^{Advill} (red columns/boxes) N shown as littermate/Nav1.7^{Advill}. **(a)** TTX-sensitive and TTX-resistant inward sodium currents recorded from Nav1.7^{Advill} DRG neurons ($N=11/6$). Current-voltage relationships for sodium currents in littermate control ($N=11$) and Nav1.7^{Advill} DRG neurons ($N=6$) in the presence **(b)** or absence **(c)** of 500 nM TTX. **(d)** WDR spinal recording from Nav1.7^{Advill} and littermate mice in response to electrical stimulation of the sciatic nerve ($N=6$ per group). **(e)** Electrically evoked substance P release into the dorsal horn measured by radioimmunoassay in Nav1.7^{Advill} and littermate mice ($N=7/8$). **(f)** First and second phase responses observed in Nav1.7^{Advill} mice after intraplantar injection of 20 μ l of 5% formalin ($N=6/5$). All data analysed by two-way analysis of variance followed by the Bonferroni *post hoc* test. Results are presented as mean \pm s.e.m. * $P < 0.05$, ** $P < 0.01$ and *** $P < 0.001$ (individual points).

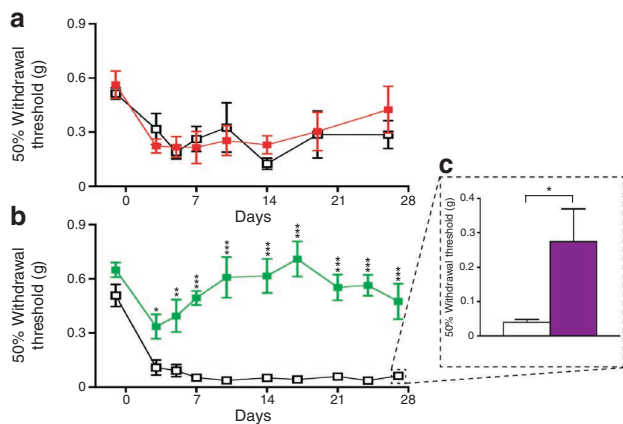


Figure 6 | Behavioural responses of Nav1.7^{Advill} and Nav1.7^{Wnt1} mice following L5 SNT. **(a)** Mechanical sensitization following L5 SNT of Nav1.7^{Advill} (red boxes, $N=6$) and littermate (white boxes, $N=9$) mice. **(b)** Mechanical sensitization following L5 SNT of Nav1.7^{Wnt1} (green boxes, $N=9$) and littermate (white boxes, $N=12$) mice. **(c)** Mechanical sensitization in littermate mice treated with 6-OHDA (purple column, $N=6$) or vehicle (white column, $N=6$) 28 days after L5 SNT surgery. All analysed by two-way analysis of variance followed by the Bonferroni *post hoc* test. Results are presented as mean \pm s.e.m. * $P < 0.05$, ** $P < 0.01$ and *** $P < 0.001$ (individual points).

conditions such as arthritis. It has been established that Nav1.7 expressed in Nav1.8-positive neurons has an essential role in inflammatory pain. Interestingly, thermal hyperalgesia, but not threshold noxious heat sensing, is mediated by Nav1.7 in the Nav1.8-positive population. This observation confirms that distinct cells and wiring patterns are associated with acute and sensitized thermosensation²¹. Figure 7 summarizes the relationship between different types

of pain sensation and the expression patterns of sodium channels Nav1.7 and Nav1.8.

One of the least understood and most problematic aspects of pain remains neuropathic pain. This may be because a variety of different mechanisms sensitize pain pathways after nerve damage. Nav1.7 expressed in Nav1.8-positive nociceptors is not required for the development of neuropathic pain in mouse models¹¹, and the studies reported here show that Nav1.7 deletion in all sensory neurons also does not significantly impair the development of neuropathic pain. As the number of CIP patients is very limited, there is no information on the importance of Nav1.7 for the development of neuropathic pain in humans. We wondered if Nav1.7 in the sympathetic nervous system contributed to neuropathic pain, as early studies in rodents³³ had made a compelling case for a sympathetic contribution to this type of pain. Interestingly, ablation of Nav1.7 in both sensory and sympathetic neurons markedly diminished neuropathic pain in the SNT model investigated here^{29,30}. This observation demonstrates an interaction between sympathetic and sensory neurons to produce neuropathic pain that is represented schematically in Fig. 7. Interestingly, pain behaviour evoked by the hotplate test is also dependent on Nav1.7 in sympathetic and sensory neurons. Behavioural responses to the hotplate test have been shown to be supraspinally integrated^{22,23,34}. A number of experimental manipulations specifically affect the hotplate behavioural response, but not reflex heat-evoked behaviour (typically tail-flick)^{34–37}. Animals in which nerve growth factor (NGF) depletion leads to loss of sensory and sympathetic neurons also show a loss of hotplate sensitivity while mechanical thresholds and thermal reflex behaviour are unaffected³⁸. NGF is not required for the survival of parasympathetic neurons³⁹. This is consistent with a role for sympathetic neurons rather than other autonomic neurons in this pain behaviour. Silencing sympathetic and some sensory neurons by deleting VGLUT2 with Cre recombinase driven by the tyrosine hydroxylase promoter also causes a loss of hotplate sensitivity while acute mechanical pain remains intact⁴⁰. In contrast, selectively

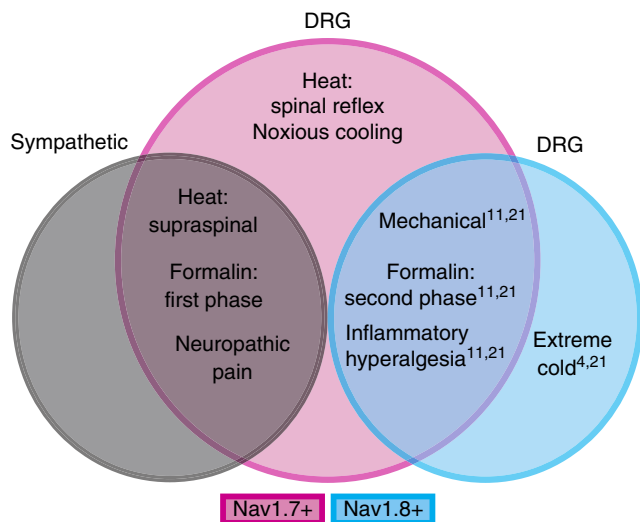


Figure 7 | The neuron-specific role of Nav1.7 in different pain states.

Nav1.7 expressed in Nav1.8-positive sensory neurons (blue) is required for mechanical pain as well as inflammatory thermal and mechanical hyperalgesia^{11,21}. Nav1.7 expressed in Nav1.8-negative neurons (red) is required for thermal acute pain sensing (but not extreme cold, which is dependent on Nav1.8^{4,21}). A contribution of both sensory and sympathetic (grey) Nav1.7-mediated signalling is required for neuropathic pain and responses to the hotplate test.

deleting VGLUT2 using Nav1.8-Cre results in a behavioural phenotype where mechanical pain behaviour is lost while thermal pain remains intact⁴¹. These findings directly mirror the behavioural phenotypes associated with selective deletion of Nav1.7 within different neuronal subpopulations (Fig. 7).

The role of the sympathetic nervous system in pain pathways has been confirmed in some rat models of neuropathic pain³³. Clinical studies have also shown a role for the sympathetic nervous system in acute human pain, for example, post-surgical pain⁴². General interest in the role of the sympathetic nervous system in pain pathways has diminished because sympathetic block has little effect in many human studies²⁶. Our results suggest that a combination of sensory and sympathetic block may prove to be more effective in treating some pain states than a sensory block alone, perhaps because complete sensory block may be hard to achieve. How sympathetic and sensory neurons interact to enhance pain sensations is unclear; interactions at nerve terminals, cell bodies and centrally have all been invoked as possible mechanisms⁴³. Interactions between sympathetic neurons and the neuronal somata of DRG neurons (Dogiel's arborizations) have been described in normal animals since the era of Ramón y Cajal⁴⁴. Sprouting and specific interactions with sensory neurons by sympathetic neurons have been observed in several chronic pain models and recently quantitated with reporter mice⁴⁵. Complex regional pain syndrome characterized by chronic burning pain and flushing in limbs supports the view that sympathetic input may contribute to pain, although the role of Nav1.7 has not been explored in this condition²⁶.

How do these findings relate to known human Nav1.7-dependent pain pathologies? It is striking that the principal sensation associated with all gain-of-function Nav1.7 mutations is burning pain. A possible explanation for this is that the heat-sensing subset of Nav1.7-expressing (Nav1.8 negative) sensory neurons show lower thresholds of activation than the Nav1.7-expressing Nav1.8-positive set of classical nociceptors linked to noxious mechanosensation. Interestingly, sympathetic block is effective in the treatment of some

erythromelalgia cases, consistent with a contribution by sympathetic neurons to acute heat sensing (Bang *et al.*⁴⁶ and references therein). Overexpression studies of gain-of-function Nav1.7 erythromelalgia-associated mutant channels in SCG neuronal somata have shown diminished excitability of sympathetic neurons, although it is unclear if lower physiological levels of Nav1.7 expression also silence sympathetic neurons.⁸

PEPD is also characterized by a burning pain evoked principally by mechanical stimuli. The association of PEPD with paroxysms of rectal, ocular or sub-mandibular pain with flushing could be related to the sympathetic contribution to this condition.² The Harlequin-like nature of flushing also implicates the autonomic nervous system (see, for example, Drummond and Lance⁴⁷). Age-related alterations in autonomic nervous system function could also be a factor in time of onset of primary erythromelalgia, which is remarkably variable in different patients⁴⁸. Finally, the ability to abolish all pain modalities in mice that fail to express Nav1.7 in the periphery provide a useful model of CIP for mechanistic studies, and confirms the utility of mouse models of human disease for mechanistic studies. These data confirm the potential of Nav1.7 as an analgesic drug target not only for acute and inflammatory pain but also for neuropathic pain.

Methods

Cre expression. Cre expression was visualized using Rosa26 floxed-stop β -galactosidase reporter mice¹⁸. Tissues were removed and stained as described previously⁴⁹. Briefly, animals were terminally anaesthetized using sodium pentobarbitone (Rhône Mérieux), before the thoracic cavity was opened, the right atrium nicked and the animal perfused, via the left ventricle, with 20 ml of ice-cold PBS followed by 20 ml of ice-cold 4% paraformaldehyde (PFA) in PBS. Organs were removed from their surrounding tissue, rinsed in PBS and fixed in ice-cold 4% PFA for 10–60 min. All tissues were stored in 30% sucrose + 0.02% sodium azide at 4°C before sectioning. Slides were washed in PBS before overnight staining with X-gal solution (5 mM potassium ferricyanide, 5 mM potassium ferrocyanide, 2 mM MgCl₂ and 0.5 mg ml⁻¹ X-gal in dimethyl formamide in PBS) at 35°C. Slides were washed three times in PBS before mounting.

Genotyping. Genomic DNA was isolated from ear or DRG. Nav1.7 was detected by PCR as described previously¹¹. The primers used were the following:

Advillin wild-type (480 bp) and Advillin-Cre (180 bp) fragments

- 5'-CCCTGTTCACTGTGAGTAGG-3' (Advillin forward)
- 5'-AGTATCTGGTAGGTGCTTCCAG-3' (Advillin wild-type reverse)
- 5'-GCGATCCCTGAACATGTCCATC-3' (Advillin-Cre reverse).

Wnt1-Cre fragment (629 bp)

- 5'-ATCCGAAAAGAAAACGTTGA-3' (forward)
- 5'-ATCCAGTTACGGATATAGT-3' (reverse).

Nav1.7 wild-type fragment (317 bp), Nav1.7 floxed fragment (461 bp) and Nav1.7 knockout fragment (395 bp)

- 5'-CAGAGATTCTGCATTAGAATTTGTTC-3' (Nav1.7 forward)
- 5'-AGTCTTTGTGGCACACGTTACCTC-3' (Nav1.7 wild-type/floxed reverse)
- 5'-GTTCTCTCTTTGAATGCTGGGCA-3' (Nav1.7 knockout reverse).

Behavioural experiments. All tests were approved by the United Kingdom Home Office Animals (Scientific Procedures) Act 1986. Experiments were conducted using both male and female wild-type littermate and knockout mice, all of which were at least 6 weeks old when tested. Observers who performed behavioural experiments were blind to the genotype of the animals. The production of the SCN9A floxed mice has been described earlier¹¹; Nav1.8-Cre mice are described in Stirling *et al.*⁴⁹; Wnt1-Cre mice are described in Danielian *et al.*¹⁶ Advillin reporter mice are described in Hasegawa *et al.*¹² and Advillin-Cre mice in Zhou *et al.*¹⁴ Nav1.8 global knockout mice were described in Akopian *et al.*⁵⁰

Motor coordination, thermal and mechanical nociceptive, was assessed as described previously^{11,51}. Briefly, animals were acclimatized to the test chambers before testing. **Rotarod:** Animals were placed onto the Rotarod at 4 r.p.m., which was then accelerated to a maximum of 40 r.p.m. within 90 s, with a cutoff of 120 s. **Hargreaves' thermal test:** The animal's hindpaw was exposed to an intense light beam and the withdrawal latency recorded. **Hotplate:** Animals were exposed to either a 50°C or a 55°C chamber floor and the withdrawal latency recorded. Thermal Place Preference (BioSeb, France) was used to assess cold avoidance. **Von Frey:** The up-down method described by Chaplan *et al.*⁵² was used to

determine a 50% response threshold. *Randall–Selitto test*: A blunt probe was used to apply force approximately midway along the tail.

Formalin test. Twenty microlitres of 5% formalin was injected into the hindpaw (intraplantar). Spontaneous nocifensive behavioural responses were recorded for 60 min post injection.

Neuropathic pain model. A modified version of the Kim and Chung³¹ model of peripheral neuropathy was adapted for use on mice^{29,30}. Thermal and mechanical thresholds were recorded at baseline and up to 28 days post surgery.

Chemical sympathectomy. 6-OHDA (Sigma) was dissolved in sterile saline containing 0.01% (w/v) ascorbic acid (vehicle) and was injected intraperitoneally at a concentration of 200 mg kg⁻¹ (ref. 53). Control mice received an equivalent volume of vehicle alone. To verify the effectiveness of this treatment in depleting norepinephrine, spleens were collected and analysed for the presence of norepinephrine by mass spectrometry.

Spinal cord electrophysiology. *In vivo* electrophysiological recordings were obtained from single WDR neurons in lamina V within the L3–L5 region of the spinal cord of anaesthetized mice⁵⁴. Neuronal activity in response to a train of 16 electrical stimuli (2 ms wide pulses at 0.5 Hz), delivered transcutaneously by means of pins inserted into the hindpaw, was recorded. Von Frey filaments and heated water jets were applied to the hindpaw for a period of 10 s to evoke mechanical and thermal nociceptive responses, respectively.

The release of substance P from dorsal horn slices was measured as described previously⁵⁵. Briefly, the lumbosacral spinal cord was excised and longitudinally hemisected, producing a horizontal slice with L4 and L5 dorsal roots attached. One slice was obtained from each animal, mounted in the central compartment of a three-compartment chamber and continuously superfused (1 ml min⁻¹) with oxygenated (95% O₂ + 5% CO₂) Krebs' solution (in mol l⁻¹: NaCl, 118; KCl, 4; MgSO₄, 1.2; KH₂PO₄, 1.2; NaHCO₃, 25; CaCl₂, 2.5 and glucose, 11) containing 0.1% BSA, 20 µg ml⁻¹ bacitracin, 100 µM captopril, 1 µM phosphoramidon and 6 µM dithiothreitol (Sigma, UK). BSA and protease inhibitors were added to minimize loss of detectable substance P through surface adhesion and to prevent degradation. The dorsal roots were then electrically stimulated (20 V, 0.5 ms, 1 Hz for 8 min). Superfusates were concentrated using C18 Sep-Pak reverse phase silica gel cartridges (Waters Associates, Watford, UK) and substance P measured by radioimmunoassay.

Statistics. Data were analysed using the GraphPad Prism 4. Student's *t*-test (two-tailed) was used for comparison of difference between two distributions. Multiple groups were compared using one-way or two-way analysis of variance with the Bonferroni *post hoc* test.

Immunocytochemistry. DRGs were excised from animals, fresh frozen in optimal cutting temperature compound (OCT), sectioned and post-fixed in 4% PFA for 5 min and then washed in PBS containing 30% sucrose. Serial 10-µm sections were mounted on sequential slides and air-dried for at least 2 h at room temperature. Slides were washed in PBS + 0.3% Triton X-100, blocked in 10% goat serum in PBS + 0.3% Triton for 1 h at room temperature and incubated in the primary antibody, diluted in the same blocking solution, overnight at 4 °C. After washing in PBS + 0.3% Triton X-100, bound primary antibodies were detected by incubating with the secondary antibody at room temperature for 2 h. The slides were then washed in PBS + 0.3% Triton X-100 and mounted using aqueous mounting solution. The following primary antibodies were used:

- Peripherin, immunoglobulin G (IgG) mouse monoclonal anti-peripherin (Sigma, UK, P-5117), 1:1,000 dilution.
- N200, IgG rabbit anti-neurofilament 200 (Sigma, UK, N4142), 1:200 dilution.

The following secondary antibodies were used:

- Alexa594, monoclonal goat anti-rabbit IgG (Invitrogen, UK, 11037), 1:1,000 dilution.
- Alexa488, monoclonal goat anti-mouse IgG (Invitrogen, UK, A11017), 1:1,000 dilution.

PCR analysis of mRNA. Total RNA was isolated from DRG. Reverse transcription was performed with 1 µg of RNA by using the iScript Select cDNA synthesis kit (Bio-Rad, catalogue #170–8896). The Nav1.7 wild-type fragment (1007 bp) and knockout fragment (478 bp) were detected by PCR with the following primers:

- 5-CCATGGTGGTACAGATTGCT-3 (forward)
- 5-CTTATCTCCGCAAGGGTACG-3 (reverse).

Cell culture. DRGs from all spinal levels were dissected from adult mice killed by CO₂ asphyxiation and prepared using a standard enzymatic dissociation procedure as described⁴⁹. Briefly, following incubation in a Dispase (Gibco)/collagenase (type XI, Sigma) mix for 40 min the ganglia were mechanically triturated using a 1-ml

Gilson pipette. The ganglia were centrifuged and resuspended in Dulbecco's modified Eagle's media supplemented with 10% fetal bovine serum, 1% Glutamax, 1% penicillin/streptomycin and 125 ng ml⁻¹ NGF. For electrophysiological recording, dissociated neurons were plated on 35-mm plastic dishes (Nunc, Denmark) coated with poly-L-lysine and laminin and used up to 24 h after plating.

For electrophysiological recording, dissociated neurons were plated on 35-mm plastic dishes (Nunc, Denmark) coated with poly-L-lysine and laminin and used up to 24 h after plating.

Whole-cell recording. Experiments were performed blind to genotype. The external solution contained (in mM): 35 NaCl, 105 CholineCl, 3 KCl, 1 MgCl₂, 1 CaCl₂, 10 glucose and 10 HEPES, pH adjusted to 7.3 and osmolarity to 320 osM l⁻¹ with NaOH and glucose, respectively. Pipettes were filled with a solution containing (in mM): 140 CsF, 10 NaCl, 2 MgCl₂, 0.1 CaCl₂, 1.1 EGTA, 10 HEPES, pH adjusted to 7.2 and osmolarity to 310 osM with CsOH and glucose, respectively. Pipette resistances were 1.8–2.5 MΩ when filled with internal solution and pipette tips were coated in Sylgard to reduce capacitance. Recordings were made at room temperature (20–22 °C).

Data acquisition and analysis. Data were acquired and analysed using the pClamp software (version 8.0; Axon Instruments). Currents were recorded from small cells (< 25 µm) using an Axopatch (200 series) patch clamp amplifier, filtered at 5 kHz and sampled at 20 kHz. The series resistance was compensated (60–75%).

Cells were depolarized to a variety of potentials (–80 to +40 mV) from a holding potential of –120 mV. The TTX-sensitive sodium current was determined as the current that was sensitive to block by 500 nM TTX and was obtained by digitally subtracting the TTX-resistant component from the total inward current. The current density was obtained by dividing the peak current by the cell capacitance as read from the amplifier. Current densities were obtained by dividing the current at each potential by the cell capacitance as read from the amplifier.

References

1. Momin, A. & Wood, J. N. Sensory neuron voltage-gated sodium channels as analgesic drug targets. *Curr. Opin. Neurobiol.* **18**, 383–388 (2008).
2. Dib-Hajj, S. D., Yang, Y. & Waxman, S. G. *Advances in Genetics* **63**, 85–110 (Elsevier, 2008).
3. Cox, J. J. *et al.* An SCN9A channelopathy causes congenital inability to experience pain. *Nature* **444**, 894–898 (2006).
4. Zimmermann, K. *et al.* Sensory neuron sodium channel Nav1.8 is essential for pain at low temperatures. *Nature* **447**, 855–858 (2007).
5. Ostman, J. A. R., Nassar, M. A., Wood, J. N. & Baker, M. D. GTP up-regulated persistent Na⁺ current and enhanced nociceptor excitability require Nav1.9. *J. Physiol.* **586**, 1077–1087 (2008).
6. Yang, Y. *et al.* Mutations in SCN9A, encoding a sodium channel alpha subunit, in patients with primary erythromelgia. *J. Med. Genet.* **41**, 171–174 (2004).
7. Dib-Hajj, S. D. *et al.* Gain-of-function mutation in Nav1.7 in familial erythromelgia induces bursting of sensory neurons. *Brain* **128**, 1847–1854 (2005).
8. Rush, A. M. *et al.* A single sodium channel mutation produces hyper- or hypoexcitability in different types of neurons. *Proc. Natl Acad. Sci. USA* **103**, 8245–8250 (2006).
9. Fertleman, C. R. *et al.* SCN9A mutations in paroxysmal extreme pain disorder: allelic variants underlie distinct channel defects and phenotypes. *Neuron* **52**, 767–774 (2006).
10. Weiss, J. *et al.* Loss-of-function mutations in sodium channel Nav1.7 cause anosmia. *Nature* **472**, 186–190 (2011).
11. Nassar, M. A. *et al.* Nociceptor-specific gene deletion reveals a major role for Nav1.7 (PN1) in acute and inflammatory pain. *Proc. Natl Acad. Sci. USA* **101**, 12706–12711 (2004).
12. Hasegawa, H., Abbott, S., Han, B.-X., Qi, Y. & Wang, F. Analyzing somatosensory axon projections with the sensory neuron-specific Advillin gene. *J. Neurosci.* **27**, 14404–14414 (2007).
13. Ravenall, S., Gavazzi, I. & Wood, J. N. A peripheral nervous system actin-binding protein regulates neurite outgrowth. *Eur. J. Neurosci.* **15**, 281–290 (2002).
14. Zhou, X. *et al.* Deletion of PIK3C3/Vps34 in sensory neurons causes rapid neurodegeneration by disrupting the endosomal but not the autophagic pathway. *Proc. Natl Acad. Sci. USA* **107**, 9424–9429 (2010).
15. Le Douarin, N. *The Neural Crest* 756 (Humana Pr Inc., New York, 1999).
16. Danielian, P. S., Muccino, D., Rowitch, D. H., Michael, S. K. & McMahon, A. P. Modification of gene activity in mouse embryos in utero by a tamoxifen-inducible form of Cre recombinase. *Curr. Biol.* **8**, 1323–1326 (1998).
17. Toledo-Aral, J. J. *et al.* Identification of PN1, a predominant voltage-dependent sodium channel expressed principally in peripheral neurons. *Proc. Natl Acad. Sci. USA* **94**, 1527–1532 (1997).
18. Soriano, P. Generalized lacZ expression with the ROSA26 Cre reporter strain. *Nat. Genet.* **21**, 70–71 (1999).

19. Jones, B. J. & Roberts, D. J. A rotarod suitable for quantitative measurements of motor incoordination in naive mice. *Naunyn Schmiedeberg's Arch. Exp. Pathol. Pharmacol.* **259**, 211 (1968).
20. Chen, C. L. *et al.* Runx1 determines nociceptive sensory neuron phenotype and is required for thermal and neuropathic pain. *Neuron* **49**, 365–377 (2006).
21. Abrahamsen, B. *et al.* The cell and molecular basis of mechanical, cold, and inflammatory pain. *Science* **321**, 702–705 (2008).
22. Le Bars, D., Gozariu, M. & Cadden, S. W. Animal models of nociception. *Pharmacol. Rev.* **53**, 597–652 (2001).
23. Langerman, L., Zakowski, M. I., Piskoun, B. & Grant, G. J. Hot plate versus tail flick: evaluation of acute tolerance to continuous morphine infusion in the rat model. *J. Pharmacol. Toxicol. Methods* **34**, 23–27 (1995).
24. Wei, H. *et al.* The influence of chemical sympathectomy on pain responsiveness and alpha 2-adrenergic antinociception in neuropathic animals. *Neuroscience* **114**, 655–668 (2002).
25. Raouf, R. *et al.* Sodium channels and mammalian sensory mechanotransduction. *Mol. Pain* **8**, 21 (2012).
26. Herrero, J. F., Laird, J. M. & López-García, J. A. Wind-up of spinal cord neurones and pain sensation: much ado about something? *Prog. Neurobiol.* **61**, 169–203 (2000).
27. Ohkubo, T., Shibata, M., Takahashi, H. & Inoki, R. Roles of substance P and somatostatin on transmission of nociceptive information induced by formalin in spinal cord. *J. Pharmacol. Exp. Ther.* **252**, 1261–1268 (1990).
28. Ghelardini, C. *et al.* Effects of a new potent analog of tocainide on hNav1.7 sodium channels and *in vivo* neuropathic pain models. *Neuroscience* **169**, 863–873 (2010).
29. Mabuchi, T. *et al.* Attenuation of neuropathic pain by the nociceptin/orphanin FQ antagonist JTC-801 is mediated by inhibition of nitric oxide production. *Eur. J. Neurosci.* **17**, 1384–1392 (2003).
30. Mabuchi, T. *et al.* Pituitary adenylate cyclase-activating polypeptide is required for the development of spinal sensitization and induction of neuropathic pain. *J. Neurosci.* **24**, 7283–7291 (2004).
31. Kim, S. H. & Chung, J. M. An experimental model for peripheral neuropathy produced by segmental spinal nerve ligation in the rat. *Pain* **50**, 355–363 (1992).
32. Muroi, Y. *et al.* Selective silencing of Nav1.7 decreases excitability and conduction in vagal sensory neurons. *J. Physiol.* **23**, 5663–5676 (2011).
33. Kim, S. H. & Chung, J. M. Sympathectomy alleviates mechanical allodynia in an experimental animal model for neuropathy in the rat. *Neurosci. Lett.* **134**, 131–134 (1991).
34. Suh, H. H., Fujimoto, J. M. & Tseng, L. L. F. Differential mechanisms mediating β -endorphin- and morphine-induced analgesia in mice. *Eur. J. Pharmacol.* **168**, 61–70 (1989).
35. Baumeister, A. & Frye, G. Involvement of the midbrain reticular-formation in self-injurious-behavior, stereotyped behavior, and analgesia induced by intranigral microinjection of muscimol. *Brain Res.* **369**, 231–242 (1986).
36. Jensen, T. S. & Yaksh, T. L. I. Comparison of antinociceptive action of morphine in the periaqueductal gray, medial and paramedial medulla in rat. *Brain Res.* **363**, 99–113 (1986).
37. Yang, C. Y., Wu, W. H. & Zbuzek, V. K. Antinociceptive effect of chronic nicotine and nociceptive effect of its withdrawal measured by hot-plate and tail-flick in rats. *Psychopharmacology* **106**, 417–420 (1992).
38. Hoffman, E. M., Zhang, Z., Anderson, M. B., Schechter, R. & Miller, K. E. Potential mechanisms for hypoalgesia induced by anti-nerve growth factor immunoglobulin are identified using autoimmune nerve growth factor deprivation. *Neuroscience* **193**, 452–465 (2011).
39. Allsopp, T. E., Robinson, M., Wyatt, S. & Davies, A. M. Ectopic trkA expression mediates a NGF survival response in NGF-independent sensory neurons but not in parasympathetic neurons. *J. Cell Biol.* **123**, 1555–1566 (1993).
40. Lagerström, M. C. *et al.* VGLUT2-dependent sensory neurons in the TRPV1 population regulate pain and itch. *Neuron* **68**, 529–542 (2010).
41. Lagerström, M. C. *et al.* A sensory subpopulation depends on vesicular glutamate transporter 2 for mechanical pain, and together with substance P, inflammatory pain. *Proc. Natl Acad. Sci. USA* **108**, 5789–5794 (2011).
42. McDonnell, J. G., Finnerty, O. & Laffey, J. G. Stellate ganglion blockade for analgesia following upper limb surgery. *Anaesthesia* **66**, 611–614 (2011).
43. Jänig, W. & Häbler, H. J. Sympathetic nervous system: contribution to chronic pain. *Prog. Brain Res.* **129**, 451–468 (2000).
44. García-Poblete, E. *et al.* Sympathetic sprouting in dorsal root ganglia (DRG): a recent histological finding? *Histol. Histopathol.* **18**, 575–586 (2003).
45. Xie, W., Strong, J. A., Mao, J. & Zhang, J. M. Highly localized interactions between sensory neurons and sprouting sympathetic fibers observed in a transgenic tyrosine hydroxylase reporter mouse. *Mol. Pain* **7**, 53 (2011).
46. Bang, Y. J., Yeo, J. S., Kim, S. O. & Park, Y. H. Sympathetic block for treating primary erythromelalgia. *Korean J. Pain* **23**, 55–59 (2010).
47. Drummond, P. D. & Lance, J. W. Site of autonomic deficit in harlequin syndrome: local autonomic failure affecting the arm and the face. *Ann. Neurol.* **34**, 814–819 (1993).
48. Pfeifer, M., Weinberg, C., Cook, D. & Best, J. Differential changes of autonomic nervous system function with age in man. *Am. J. Med.* **75**, 249–258 (1983).
49. Stirling, L. C. *et al.* Nociceptor-specific gene deletion using heterozygous Nav1.8-Cre recombinase mice. *Pain* **113**, 27–36 (2005).
50. Akopian, A. N. *et al.* The tetrodotoxin-resistant sodium channel SNS has a specialized function in pain pathways. *Nat. Neurosci.* **2**, 541–548 (1999).
51. Minett, M. S., Quick, K. & Wood, J. N. *Current Protocols in Mouse Biology* Vol. 1 383–412 (Hoboken, NJ, USA, 2011).
52. Chaplan, S. R., Bach, F. W., Pogrel, J. W., Chung, J. M. & Yaksh, T. L. Quantitative assessment of tactile allodynia in the rat paw. *J. Neurosci. Methods* **53**, 55–63 (1994).
53. Leo, N. A., Callahan, T. A. & Bonneau, R. H. Peripheral sympathetic denervation alters both the primary and memory cellular immune responses to herpes simplex virus infection. *Neuroimmunomodulation* **5**, 22–35 (1998).
54. Harvey, V. L. & Dickenson, A. H. Behavioural and electrophysiological characterisation of experimentally induced osteoarthritis and neuropathy in C57Bl/6 mice. *Mol. Pain* **5**, 18 (2009).
55. Lever, I. J. *et al.* Basal and activity-induced release of substance P from primary afferent fibres in NK1 receptor knockout mice: evidence for negative feedback. *Neuropharmacology* **45**, 1101–1110 (2003).

Acknowledgements

We thank the BBSRC and the MRC/Pfizer for their support. J.N.W., A.H.D. and M.S.M. are members of the Wellcome Trust-funded London Pain Consortium. J.N.W. was also supported by Grant No. R31-2008-000-10103-0 from the World Class University Programme (WCU) project of the National Research Foundation (NRF) at the Seoul National University. We thank James Cox, Niels Eijkelkamp, Jing Zhao and other members of the lab for useful critical comments and technical advice.

Author contributions

MSM carried out behavioural experiments and *in vivo* electrophysiology on transgenic mouse lines, MN and FW provided mouse lines and advice, AC and MM carried out substance P release experiments, GP carried out electrophysiology experiments, AHD provided equipment and advice. JNW and MSM conceived the study and wrote the manuscript that was edited by all other co-authors.

Additional information

Supplementary Information accompanies this paper at <http://www.nature.com/naturecommunications>

Competing financial interests: The authors declare no competing financial interests.

Reprints and permission information is available online at <http://npg.nature.com/reprintsandpermissions/>

How to cite this article: Minett, M.S. *et al.* Distinct Nav1.7-dependent pain sensations require different sets of sensory and sympathetic neurons. *Nat. Commun.* **3**:791 doi: 10.1038/ncomms1795 (2012).

License: This work is licensed under a Creative Commons Attribution-NonCommercial-NoDerivative Works 3.0 Unported License. To view a copy of this license, visit <http://creativecommons.org/licenses/by-nc-nd/3.0/>